

# Flexible acrylate-grafted silica aerogels for insulation purposes: comparison of reinforcement strategies

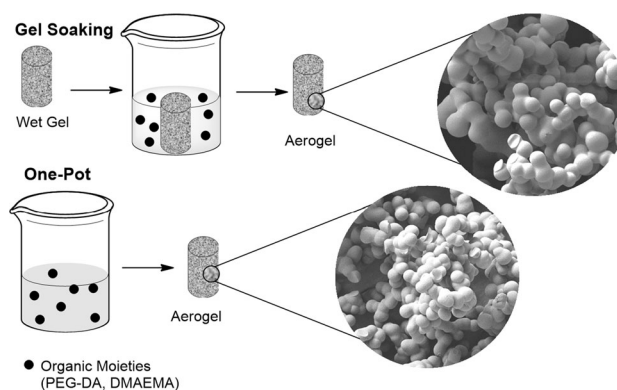
João P. Vareda<sup>1</sup> · Telma Matias<sup>1</sup> · Ana C. Fonseca<sup>2</sup> · Luisa Durães<sup>1</sup>

Received: 4 March 2016 / Accepted: 26 June 2016  
© Springer Science+Business Media New York 2016

**Abstract** Vinyltrimethoxysilane (VTMS), methyltrimethoxysilane (MTMS) and tetramethylorthosilicate (TMOS) were mixed in a one-step basic catalyzed sol-gel chemistry, to produce flexible and good thermal insulator silica-based aerogels. Moreover, mechanical reinforcement of the aerogels with a polymer phase was accomplished via free radical polymerization using either the macromer poly(ethylene glycol) diacrylate (PEG-DA) or the monomer 2-(dimethylamino)ethyl methacrylate (DMAEMA), the latter case resulting in the grafting of PDMAEMA. Both the influence of using a monomer or a macromer and of applying two different polymer grafting approaches—one-pot synthesis or gel soaking—on the aerogels' final properties were analyzed. It was concluded that gel soaking strongly limits the diffusion of the organic moieties, creating heterogeneous materials. This approach led to denser and less hydrophobic aerogels with worse mechanical properties. The incorporation of low amounts of polymer with one-pot synthesis led to an improvement in the aerogels properties, making them less dense, more flexible and better insulators. The one-pot method also allowed to obtain aerogels with a very well-defined microstructure, due to the porogen role of the polymer, hence generating homogenous materials. It was found that the major differences in the aerogels properties occurred with different grafting approaches and not with different

polymer phases, and the molecular weight of the organic moieties was not determinant for the materials homogeneity, in the studied cases. The obtained bulk densities ranged from 122 to 181 kg m<sup>-3</sup>, the thermal conductivity from 0.050 to 0.072 W m<sup>-1</sup> K<sup>-1</sup> and the modulus achieved 327 kPa. The addition of DMAEMA generated the best results when using the one-pot approach, providing the lightest and uncommonly flexible thermal insulator aerogels (modulus of ~70 kPa).

## Graphical Abstract



**Electronic supplementary material** The online version of this article (doi:10.1007/s10971-016-4137-6) contains supplementary material, which is available to authorized users.

✉ Luisa Durães  
luisa@eq.uc.pt

<sup>1</sup> CIEPQPF, Department of Chemical Engineering, University of Coimbra, Rua Sílvio Lima, 3030-790 Coimbra, Portugal

<sup>2</sup> CEMUC, Department of Chemical Engineering, University of Coimbra, 3030-790 Coimbra, Portugal

**Keywords** Silica aerogel · Grafting · One-pot · Gel soaking · Acrylate · Thermal insulation

## 1 Introduction

Silica aerogels are highly porous, lightweight and good thermal insulator materials obtained by supercritical drying techniques [1–5]. Moreover, these materials can exhibit other excellent and unique properties, which can be

tailored using sol–gel technology. For example, methyltrimethoxysilane (MTMS)- and methyltriethoxysilane (MTES)-derived aerogels show uncommon high flexibility and hydrophobicity [3, 4, 6]. Thus, silica aerogels have been proposed for building insulation (for both thermal and acoustic insulation) [5, 6], thermal insulators for space vehicles and extra-vehicular activity [7], catalyst supports [6], supercapacitors [2] and Cherenkov radiation detectors [1], among others. Nonetheless, silica aerogels usually have weak mechanical properties that limit their handling/processing and use in load bearing applications.

Several strategies have been applied to overcome the fragile nature of silica aerogels [8]. The inclusion of flexible bis-silanes into the silica backbone, via co-gelation, has shown to reduce the Young's modulus and bulk density of the resulting aerogels when using optimized conditions [7–10]. The addition of these precursors creates a more open structure that also leads to better thermal insulation characteristics [11].

A different approach to the problem is the reinforcement of the silica structure by cross-linking with polymers, obtaining hybrid materials [8, 9, 12]. The polymeric chains grow on the modified surface of secondary particles, creating a coating and increasing the connection between them [11]. This strategy strengthens the pearl necklace structure of the mesoporous silica making it sturdier. However, this also increases the aerogel's bulk density which leads to an increased thermal conductivity [8]. Regardless of being two different approaches Nguyen et al. [13], Meador et al. [14], Maleki et al. [11] and Randall et al. [7] combined the two. The latter studied the properties obtained with different silica backbones for the same cross-linker and the effect of different cross-linkers on the properties of the same silica backbone. Randall et al. [7] concluded that larger alkyl chains in the bis-silane improved some desired properties (low bulk density, high modulus and recovery from compression), with the hexyl link being considered an optimum chain length. This combined approach allows, in theory, to improve the aerogels mechanical properties even further, and the open structure obtained in the silica backbone with the co-gelation of bis-silanes compensates, to some extension, the increasing density due to cross-linking.

Reinforcement of silica aerogels via polymer cross-linking has been widely investigated, and a variety of different cross-linkers like epoxide [7, 14, 15], poly (acrylates) [7, 8, 12, 16], polyureas [7, 8], isocyanate [7, 8, 13] and polystyrene [7–9, 12, 16] have been used for reinforcement. To create a covalent bond between the two phases, functionalization of the silica backbone is necessary and can be performed by co-gelation with a silane containing an organic reactive functional group, like vinyl or amine [8, 9, 14]. Liquid-phase polymer reinforcement,

the most frequent strategy, can be achieved in two different ways. The first consists in soaking the aged aerogel in a monomer solution prepared with a post gelation solvent. During the soaking period, the monomer molecules diffuse into the interior of the wet gel. This method is time-consuming and is limited by monomer diffusion through the highly complex pore system of the silica aerogel [8, 9, 14]. The second method, also called one-pot synthesis, is less time-consuming and more straightforward, with the organic moieties being added to the sol along with the silica precursors. With this strategy, the monomer molecules are entrapped inside the porous structure. Afterward, for both cases, the reaction between the monomer and functionalized silica is promoted by a heat stimulus and the resulting hybrid wet gel is dried [8, 11, 15].

In this study, we test the polymer reinforcement of silica-based aerogels obtained from the co-gelation of vinyltrimethoxysilane (VTMS), trimethoxymethylsilane (MTMS) and tetramethylorthosilicate (TMOS). With the used mixture of silane alkoxides, we intend to synthesize flexible and hydrophobic aerogels, in a one-step basic catalysis, which also include organic moieties (vinyl groups) that can react with the monomers via free radical polymerization. Poly(ethylene glycol) diacrylate (PEG-DA) and 2-(dimethylamino)ethyl methacrylate (DMAEMA) were studied as macromer and monomer for polymer reinforcement. The different molecular weight will influence monomer diffusion in gel soaking methodology and the porogen effect in one-pot synthesis. Since PEG-DA is highly hydrophilic, it is important to maintain it in low amount to not compromise the hydrophobicity of the final material. Monoliths obtained with both gel soaking and one-pot synthesis are compared in order to determine the most efficient method for the manufacturing of monoliths for insulation-related applications. Key properties of the aerogels for these applications, such as bulk density (porosity), thermal conductivity, flexibility and hydrophobicity, were evaluated.

## 2 Experimental

### 2.1 Materials

Vinyltrimethoxysilane (VTMS, 98 %,  $\text{H}_2\text{C}=\text{CHSi}(\text{OCH}_3)_3$ ), methyltrimethoxysilane (MTMS, 98 %,  $\text{CH}_3\text{Si}(\text{OCH}_3)_3$ ), tetramethylorthosilicate (TMOS,  $\geq 98$  %,  $\text{Si}(\text{OCH}_3)_4$ ), poly(ethyleneglycol diacrylate) (PEG-DA, Mn  $\sim 575$ ,  $\text{H}_2\text{C}=\text{CHCO}(\text{OCH}_2\text{CH}_2)_n\text{OCOCH}=\text{CH}_2$ ), 2-(dimethylamino)ethyl methacrylate (DMAEMA,  $\text{CH}_2=\text{C}(\text{CH}_3)\text{COOCH}_2\text{CH}_2\text{N}(\text{CH}_3)_2$ ), methanol ( $\geq 99.8$  %,  $\text{CH}_3\text{OH}$ ), tetrahydrofuran (THF,  $\geq 99.9$  %,  $\text{C}_4\text{H}_8\text{O}$ ), ammonium hydroxide (25 % wt,  $\text{NH}_4\text{OH}$ ) and 2,2'-azobis(2-methylpropanitrile)

(AIBN,  $\approx 98\%$ ,  $(\text{CH}_3)_2\text{C}(\text{CN})\text{N}=\text{NC}(\text{CH}_3)_2\text{CN}$ ) were purchased from *Sigma-Aldrich*. Only DMAEMA was purified prior to utilization by passing it over a silica–alumina column.

## 2.2 Synthesis of the silica backbone

Preliminary tests were conducted in order to optimize the silica precursors' mixture. Selection criteria included complete gelation of the mixture, bulk density and monolithicity [17].

A solution consisting of VTMS (40 mol%), MTMS (40 mol%) and TMOS (20 mol%) in methanol was stirred at  $0\text{ }^\circ\text{C}$  in an ice/ethanol bath. A 1 M aqueous solution of ammonium hydroxide was prepared separately and added to the first one. Typically, for 100 mL of gel, 1 mL of ammonium hydroxide solution (25 % in water) was added to the precursors' mixture, keeping a total silicon concentration of 1.82 M and a water/silicon molar ratio of 7.8. The resulting mixture was homogenized for a few seconds, then, poured in cylindrical poly(propylene) molds and left for aging at  $27\text{ }^\circ\text{C}$  for 48 h.

## 2.3 Polymer reinforcement via gel soaking

After the aging period, the silica alcogels were unmolded and dipped in a new solution made of a post-gelation solvent (THF), the monomer/macromer to be grafted and AIBN, with 50 % (w/w) monomer/macromer to THF. The amount of AIBN added was 3 % of monomer/macromer mass. For DMAEMA, this solution was degassed for 30 min with nitrogen. After being soaked for 72 h at room temperature, the wet gels were placed in a cylindrical reaction flask, covered with fresh THF and then refluxed for 24 h for polymerization (Fig. 1).

The amount of monomer added to the system was based on its molecular weight and prior results [17]. Table 1 features the monomer concentrations tested in the gel soaking procedure. PEG-DA already has a developed carbon chain, and for reinforcement purposes, it is not crucial that it undergoes further growing. Moreover, each molecule of this polymer has two reactive ends that can link to vinyl groups, so the PEG-DA/VTMS molar ratio was kept low, although with a slight excess to increase the concentration difference for a more efficient diffusion. On the other hand, in the case of DMAEMA, the monomer/VTMS ratio was increased in order to favor polymer chain growth.

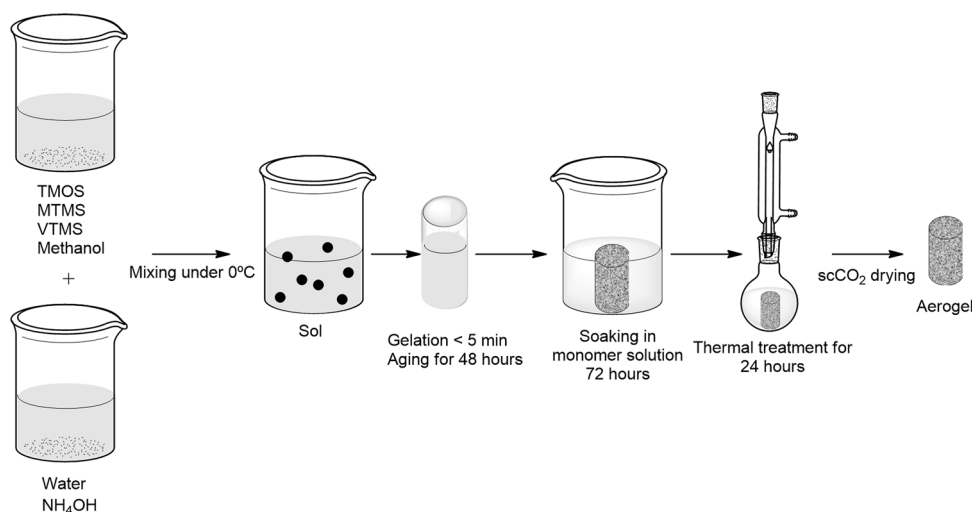
## 2.4 Preparation of reinforced gels via one-pot synthesis

An aqueous solution of ammonium hydroxide 1 M was combined with methanol, the monomer/macromer and AIBN (3 % of the monomer/macromer mass). This was added, under stirring, to a solution containing methanol and the silica precursors. After stirring, the mixture was poured into cylindrical poly(propylene) molds at room temperature for gelation and then left for aging at  $27\text{ }^\circ\text{C}$  for 48 h. After aging, the polymerization of the monomers in the gel proceeded applying THF reflux, as mentioned in Sect. 2.3 (Fig. 2).

In order to optimize the monoliths properties, some monomer concentrations were tested as there were no previous results [17]. Table 1 presents the tested monomer/VTMS molar ratios. Concentrations were varied, starting on a small monomer/VTMS molar ratio and then increased until gelation was inhibited or the resulting monolith became very rigid.

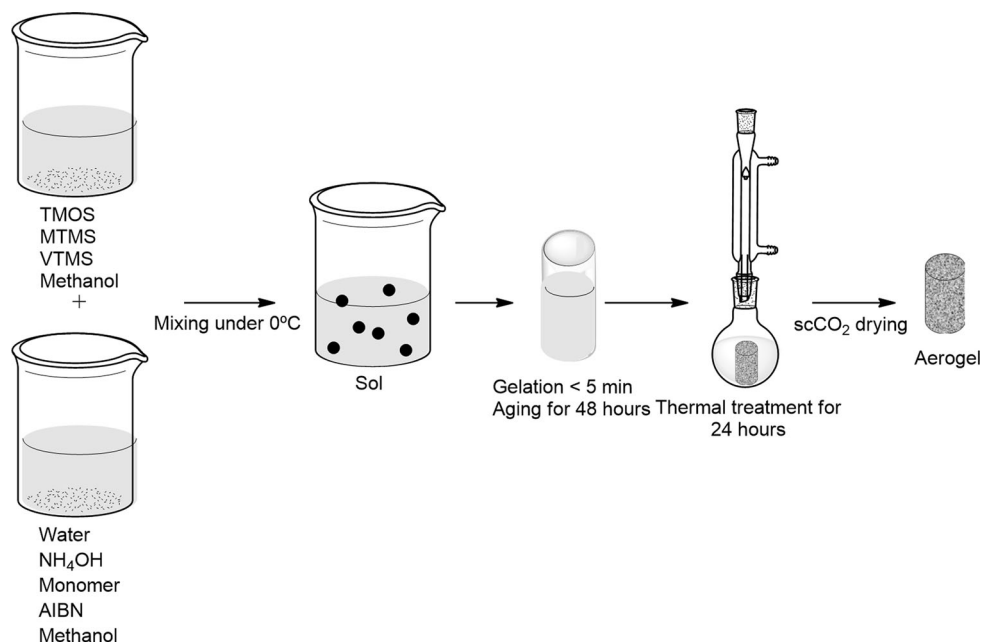
The reference sample, which is an unreinforced aerogel with the same modified silica backbone of the reinforced

**Fig. 1** Schematic representation of the experimental procedure used for grafting via gel soaking



**Table 1** Monomer/VTMS molar ratios (*R*) tested for gel soaking and one-pot approaches

Method of monomer addition	PEG-DA/VTMS (mol/mol)	Samples label	DMAEMA/VTMS (mol/mol)	Samples label
Gel soaking	1.6	A_PP_S_R1.6	10	A_PD_S_R10
One-pot	0.5	A_PP_O_R0.5	0.5	A_PD_O_R0.5
	1	A_PP_O_R1	1	A_PD_O_R1
			2	A_PD_O_R2
			5	A_PD_O_R5

**Fig. 2** Schematic representation of the experimental procedure used for grafting via one-pot

aerogels, is labeled as A\_P0. The reinforced aerogels labeling uses the following scheme: A stands for aerogel; PX identifies the type of polymer grafted in the silica network ( $X = P$ , aerogel reinforced with PEG-DA;  $X = D$ , aerogel reinforced with PDMAEMA); S means that gel soaking was used as grafting method, while O corresponds to one-pot synthesis; and the last term defines the molar ratio (*R*) between monomer and VTMS (for example, R2 means that for each vinyl group of the silica backbone there are two monomer molecules in the system).

## 2.5 Gels drying

Gels were placed in a supercritical extraction stainless steel chamber and dried via continuous supercritical fluids extraction. The gels were firstly washed with a flow of hot methanol at high pressure, and then, they were dried by extracting the methanol with supercritical CO<sub>2</sub> at 50 °C and 150 bar [18].

## 2.6 Aerogels characterization

Key properties of the aerogels were determined as follows: (1) bulk density—by weight–volume measurements of four cubic pieces of each replica; (2) porosity—calculated from bulk and skeletal densities, using Eq. (1), being the skeletal density accessed with helium pycnometry (*Accupyc 1330, Micrometrics*) carried out on previously ground samples; (3) hydrophobicity—determined via contact angle measurement (*OCA 20, Dataphysics*), using the sessile drop technique with high purity water as test liquid; (4) thermal conductivity—measurements were taken using the transient plane source method (*TPS2500 Hot Disk Thermal Constants Analyzer, Hot Disk*) and placing the sensor between the flat side of two cylindrical pieces of material with similar dimensions, at 20 °C.

$$\text{Porosity \%} = 100 \times \left( 1 - \frac{\rho_b}{\rho_s} \right) \quad (1)$$

Chemical structure of the aerogel monoliths was accessed by FTIR spectroscopy (*FT/IR 4200, Jasco*), using the KBr mode, in the range of 4000–400  $\text{cm}^{-1}$ , with a resolution of 4  $\text{cm}^{-1}$  and 64 scans.

Thermal characterization was performed by thermogravimetric analysis—TGA (*SDTQ600, TA Instruments*), using powdered samples, until a temperature of 1200 °C, at 10 °C  $\text{min}^{-1}$  in a nitrogen atmosphere.

Mechanical behavior of the monoliths was accessed applying a uniaxial compression test (*Shimadzu AG-IS 100KN*, control of the compression velocity and a *AND EK-1200i* balance) on cylindrical samples, with a speed of 1.3 mm/min.

Microstructure was observed and chemically characterized with field emission scanning electron microscope (*Compact/VPCompact FESEM, Zeiss Merlin*) and energy-dispersive X-ray spectroscopy (EDS) (*XMaxN, Oxford*), respectively.

### 3 Results and discussion

Most promising aerogels, both non-reinforced and reinforced with PEG-DA and PDMAEMA, are shown in Fig. 3. Gelation for both non-reinforced and grafted gels was rather quick, with gelation occurring within 5 min after the mixing of the basic catalyst. Three replicas of each

sample were synthesized and characterized, except for sample A\_PP\_S\_R1.6.

Non-cross-linked silica aerogels exhibited a shining, plastic look on its outer surface, and, although being relatively rigid, they were still compressible. Moreover, they show negligible particle shedding. Aerogels grafted using the gel-soaking technique have a very different aspect. The monoliths are more rigid in general, and when grafted with PEG-DA, they show heterogeneity, with rigid and soft parts, and could be easily broken. The shining look was not observed in this case, but the aerogels remained quite clean in terms of particles release. One-pot synthesis originated the most flexible monoliths. These show a dull-looking surface, and they always released powder.

It was observed that for a higher amount of polymer the aerogel's integrity improved, although there is a concentration for which the aerogel became extremely rigid.

#### 3.1 Key properties

Table 2 presents the key properties of the most promising monoliths. The mechanical properties presented in this table will be discussed only in Sect. 3.4.

It is evident that grafting via gel soaking, comparing with non-reinforced aerogels, generally creates denser

**Fig. 3** Photographs of some of the monoliths. **a** A\_P0 (non-reinforced sample); **b** A\_PP\_S\_R1.6; **c** A\_PP\_O\_R0.5; **d** A\_PD\_S\_R10; **e** A\_PD\_O\_R2

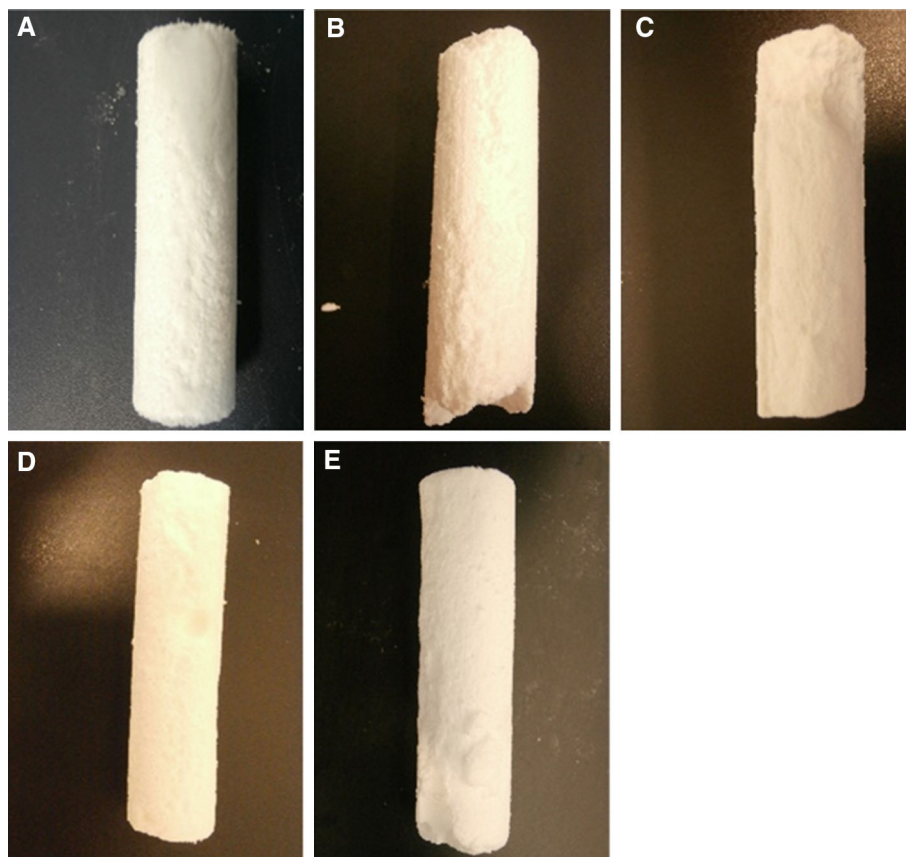


**Table 2** Key properties of selected aerogels

Sample	Bulk density (kg m <sup>-3</sup> )	Porosity (%)	Shrinkage (%) <sup>(a)</sup>	Contact angle (°)	Thermal conductivity (W m <sup>-1</sup> K <sup>-1</sup> )	Young's modulus (kPa)	Compressive strength (kPa)	Elongation at break (%)
A_PO	148.8 ± 5.6	89	13.7	144 ± 12	0.063 ± 0.004	927.5	71.3	16.37
A_PP_S_R1.6	147.5	88	5.4	112	0.072	627.1	47.0	15.50
A_PP_O_R0.5	132.7 ± 7.6	91	10.6	151 ± 6	0.061 ± 0.017	97.6	19.3	32.76
A_PD_S_R10	181.5 ± 50.5	86	12.1	122 ± 56	0.067 ± 0.022	848.4	366.6	47.82
A_PD_O_R2	122.6 ± 6.8	91	13.4	150 ± 9	0.050 ± 0.007	68.6	19.5	30.17

<sup>a</sup> Shrinkage was estimated by the bulk and theoretical densities using the formula:  $\left(1 - \frac{\rho_L}{\rho_b}\right) \times 100$

aerogels with increased thermal conductivity and decreased porosity. Porosity is related to the bulk density, being inversely proportional properties and is calculated with both bulk and skeletal densities by Eq. (1). Thus, it is influenced by the uncertainties of these two measurements and by the amount of closed pores in the structure. In this way, only averaged nominal values are presented.

Shrinkage, also presented in Table 2, was estimated using the theoretical and bulk densities of samples. For the theoretical density calculation, it was assumed that the gel skeleton mass remains constant during drying, being the theoretical mass obtained considering complete hydrolysis and condensation of silica precursors and the polymer mass percentage measured by TGA analysis. The volume of solution, hence the gel volume, was kept at 40 mL in all syntheses.

Shrinkage of the gels is fairly similar in all samples, as expected considering their monolithic appearance from Fig. 3. However, it seems that the addition of a polymer phase tends to decrease the gel's shrinkage during supercritical drying, which is more noticeable in the samples with PEG-DA. In fact, this polymer tends to cross-link, giving a more cohesive structure that hinders shrinkage. When in one-pot layout, this cross-linking is not so extensive due to the presence of the silica structure, thus giving higher shrinkage values than for the gel-soaking approach.

Thermal conductivity of aerogels, at low temperature, is mainly dependent on solid heat conduction through the silica particles and heat conduction through the gaseous phase [18, 19]. The gaseous phase can transfer heat through conduction and convection, being the latest inhibited/reduced due to the small pore dimension and complex porous network of aerogels [19]. Thus, aerogels thermal conductivity is usually the sum of the solid heat conduction and gas heat conduction [18, 19], and the latter is the limiting step. Therefore, denser aerogels tend to be worse insulators, being our results in agreement with this trend (Table 2).

The addition of the organic moieties in the sol phase (one-pot strategy) created a different aerogel structure.

Results suggest a tendency for weightless and better insulator monoliths in this case (Table 2), characteristics originated by the porogen effect of the polymer during gelation, which controls particle growth and decreases the pore size (as it will be seen later in SEM analysis), decreasing the influence of the gaseous convection but also reducing the bulk density.

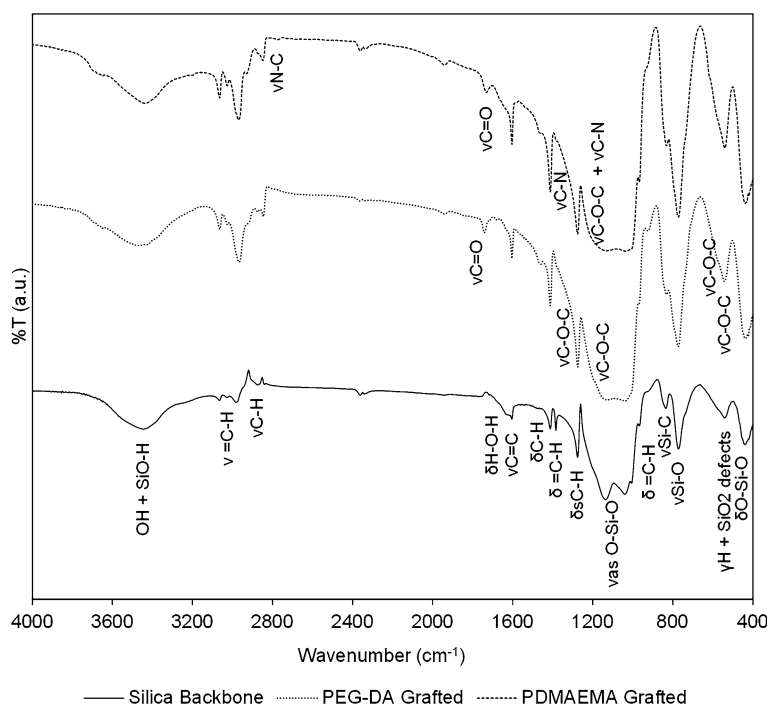
Hydrophobic monoliths are stable when exposed to moisture. Methyl and vinyl groups derived from MTMS and VTMS, respectively, turned the silica backbone hydrophobic, as shown by the high contact angle values of the synthesized aerogels (112–150°, Table 2). However, not all obtained aerogels are equally hydrophobic. Gel-soaking-grafted aerogels show a decrease in contact angle (112° and 122°), when compared to non-reinforced aerogels (A2\_PO, 144°), and thus, those were considered as being near the transition between hydrophilic and hydrophobic materials. In this type of aerogels, for PEG-DA reinforcement, the water drop was often absorbed by the test material which caused difficulties in the analyses; this was certainly due to the hydrophilic nature of PEG-DA and its heterogeneous distribution on the aerogel surface.

Grafting via one-pot retains the hydrophobic characteristics of the aerogels, probably due to a more organized porous structure provided by the porogen effect of the organic moieties, which leads to well-dispersed hydrophobic functional groups.

For both polymers, one-pot synthesis is the only grafting method that improves the discussed key properties, creating the most adequate materials, from this point of view. Moreover, it is PDMAEMA that most improves these properties, being the sample A\_PD\_O\_R2 the best one in this context.

The aerogels prepared in this study are lighter than the ones obtained with epoxy cross-linking that feature bulk densities varying from 198 to 847 kg m<sup>-3</sup> [15]. The polystyrene-grafted materials obtained by Nguyen et al. [9] also feature a wide range of bulk densities, going up to 370 kg m<sup>-3</sup>. The lightest materials obtained by these authors have similar densities to the ones achieved in this

**Fig. 4** Typical FTIR spectra for the synthesized aerogels ( $\nu$ —stretching vibration;  $\delta$ —bending vibration;  $s$ —symmetric;  $as$ —asymmetric;  $\gamma$ —out of plane bending vibration; in particular, the shown spectra are from samples A\_P0, A\_PP\_O\_R0.5 and A\_PD\_S\_R10)



publication via the one-pot method. Maleki et al. [16] grafted aerogels with poly(butyl acrylate) and polystyrene, obtaining monoliths of similar density.

In spite of having interesting insulation properties, the aerogels with polymer reinforcement presented in this paper are not yet as good insulators as MTMS-derived aerogels and aerogel-like materials [18, 20], as expected due to the much lower bulk density of the latter.

### 3.2 Chemical structure

#### 3.2.1 FTIR

Figure 4 shows the typical FTIR spectra for the synthesized aerogels, from which the characteristic functional groups were identified considering the data in the open literature [21]. The same chemical system, although with variation in the relative proportion of its components (different samples) or in the grafting method, generated similar spectra. Thus, a representative spectrum was selected to show the typical functional groups of the aerogels for each specific chemical system.

For all gels, an organically modified silica network is formed, whose chemical composition is in agreement with an aerogel derived from MTMS, VTMS and TMOS [21]. There is a predominance of siloxane (Si–O–Si) bonds, being also observed the methyl and vinyl groups incorporated therein as well as the hydroxyl groups from network ends. The characteristic vibrations of the siloxane bonds are detected at approximately  $438\text{ cm}^{-1}$  (bending),  $540\text{ cm}^{-1}$  (SiO<sub>2</sub> defects),  $771\text{ cm}^{-1}$  and between 1039 and

$1135\text{ cm}^{-1}$  (stretching). The vibrations of the methyl groups are also visible in all aerogels as this functional group is not reactive. The vibrations of the vinyl groups can be found at 540, 920, 1002, 1383, 1412, 1604, 1940, 3027,  $3065\text{ cm}^{-1}$ , while peaks representing vibrations associated with the methyl groups can be found at 835, 1276, 1412, 1477, 2839, 2875 and  $2982\text{ cm}^{-1}$ . Peaks representing the hydroxyl group are found at 1630 and  $3447\text{ cm}^{-1}$ .

For grafted aerogels, the spectra show bands that correspond to the characteristic functional groups of each polymer (C–N stretching for PDMAEMA, C–O–C stretching and C=O stretching for both polymers) that are sometimes overlapped with other peaks, but also show that the vinyl groups still exist (peak at  $1600\text{ cm}^{-1}$ ). We can conclude from this observation that the remaining vinyl groups are either from remaining active sites on the silica backbone (unreacted VTMS) or from unreacted monomer molecules. Thus, not all vinyl groups were used to create covalent bonds between the two phases. This can be due to the highly complex pore system of the aerogel, which hinders the diffusion of the organic moieties to reach the vinyl groups on the silica backbone, and also due to steric hindrance caused by the methyl groups.

### 3.3 Thermal characterization

TGA analysis was conducted for selected aerogels and grafting polymers (Fig. 5). Monomers were polymerized using the same conditions applied to the gels heat treatment, and the neat polymer was also subjected to the

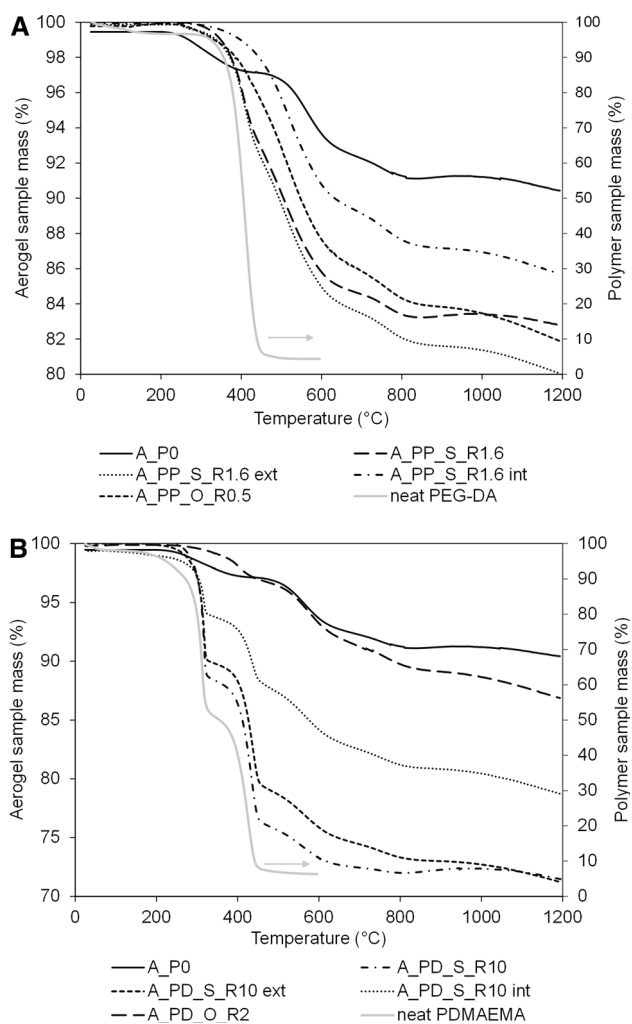


**Fig. 5** TGA curves of the synthesized aerogels; **a** PEG-DA-grafted aerogels versus non-reinforced aerogel; **b** PDMAEMA-grafted aerogels versus non-reinforced aerogel. Samples representative of the aerogels core are labeled as “int” (=interior) and of the outer surface as “ext” (=exterior)

thermal degradation analysis. Tests were ran with a sample representative of the entire aerogel (mixing the core material with that of the outer surface), but for gel-soaking-grafted aerogels, a sample representative of the core (called interior) and one from the outer surface (called exterior) were analyzed separately. Table S1 shows the stages of mass loss and respective temperature ranges. The average amount of polymer mass in each grafted aerogel was obtained running three independent tests.

Figure 5a shows that PEG-DA-grafted aerogels (A\_PP\_S\_R1.6 and A\_PP\_O\_R0.5) start to degrade at higher temperatures when compared to the non-reinforced aerogel (A\_P0) or the neat polymer itself. The covalent bonds between carbon and silicon atoms are very stable; hence, the hybrid aerogels show increased thermal stability. PEG-DA-grafted aerogels undergo significant mass

loss between 400 and 600 °C (Fig. 5a, Table S1), attributed to the polymer-phase degradation. The differences between residual masses (in relation to the non-reinforced aerogel) and the shape of the curve itself reveal the incorporation of the polymer phase in reinforced aerogels.

Representative curves of outer surface and core of the hybrid aerogels prepared by gel soaking allow understanding the efficiency of monomer diffusion through the gel and the heterogeneity of these materials. These two curves feature a significant difference in the amount of polymer, meaning that this methodology creates heterogeneous materials due to difficult monomer diffusion, as reported before [15]. It is reasonable to assume that polymer concentration in the aerogel varies in the radial direction, decreasing toward the center of the cylindrical samples. Comparing the hybrid aerogels obtained by one-pot and gel soaking strategies, it is notorious that one-pot synthesis succeeds in incorporating more PEG-DA in the aerogel ( $8.90 \pm 1.97$  % for A\_PP\_O\_R0.5 and  $7.98 \pm 0.69$  % for A\_PP\_S\_R1.6), considering that the amount of monomer added in this case was much smaller than for gel soaking.

PDMAEMA-grafted aerogels (A\_PD\_S\_R10 and A\_PD\_O\_R2) feature a similar behavior. These aerogels are also more stable than the individual phases (Fig. 5b). A significant weight loss is visible between 300 and 550 °C (Fig. 5b, Table S1), corresponding to polymer-phase degradation. Outer surface and core curves reveal that diffusional limitation and heterogeneities are still present when using a monomer. We can conclude that although less significant in PDMAEMA-grafted aerogels, the diffusional limitations also happen in gel-soaking-grafted aerogels, even with PDMAEMA's smaller molecular weight. In these aerogels, gel soaking was the methodology that allowed to incorporate more polymer into the monolith ( $2.95 \pm 1.63$  % for A\_PD\_O\_R2 one-pot and  $19.59 \pm 5.26$  % for A\_PD\_S\_R10) and this result is now clearly dependent on the amount of monomer added to the system. However, one-pot synthesis creates less heterogeneities and allows for polymer incorporation even with small amounts of organic moieties added.

### 3.4 Mechanical behavior

Not all uniaxial compression tests ended with complete breaking of the samples. Instead, the material started to peel, with fractures being created at the exterior surface, confirming the heterogeneous nature of these materials. This behavior was expected because the outer surface of the aerogels is denser, with a less open structure, due to more extensive gelation next to the solid surface of the container. Moreover, in the soaked aerogels, the amount of polymer in the outer surface is higher than the amount on

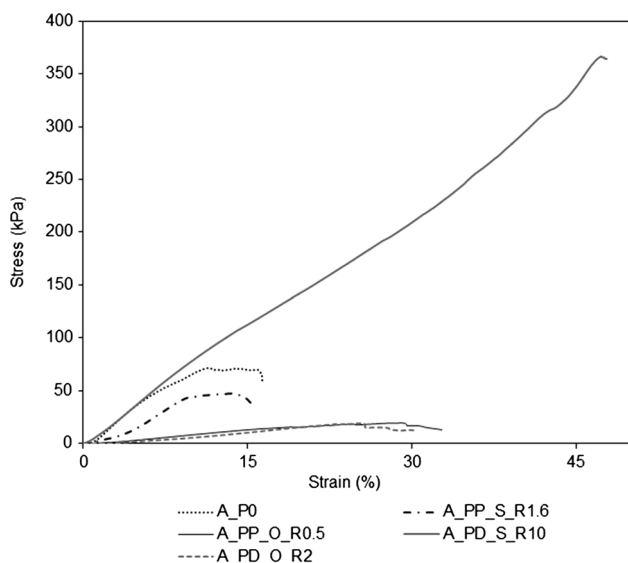


**Fig. 6** Stress–strain diagrams of the selected aerogels

its interior, which increases the rigidity of this surface. Figure 6 presents the stress–strain diagrams for the selected samples, and Table 2 summarizes the corresponding mechanical properties.

Table 2 shows that the most rigid aerogel, which has the higher value of Young's modulus, is the non-reinforced one (928 kPa). This behavior was expected because the polymer phase features covalent bonds that are much more elastic than the siloxane bonds, helping the flexibility of the structure. Although not all elastic modulus values were significantly reduced, in general polymer reinforcement decreased the materials rigidity, creating more flexible aerogels (modulus  $\leq 848$  kPa for reinforced samples). This behavior is more noticeable on aerogels grafted via one-pot (69 kPa with DMAEMA, 98 kPa with PEG-DA).

Polymer reinforcement should have also increased the compressive strength of the materials, but this fact was not observed. Because of the peeling behavior of monoliths during the test, these measurements do not give the mechanical strength of the aerogel's core part that is certainly much higher. One-pot-grafted aerogels are the ones that present the smaller compressive strength, regardless the polymer used ( $\sim 20$  kPa). The presence of the organic moieties during gelation creates more homogeneous monoliths but makes a more fragile silica structure, due to less extent of condensation. The significant mass loss after 1000 °C that these materials suffer (Fig. 5, Table S1), comparing to the others, is consistent with defects of the silica network.

Materials that are less rigid can deform more until break, and thus, polymer reinforcement should also increase the materials elongation at break. Table 2 shows that grafted aerogels have higher elongation at break (up to 48 %) than

the non-reinforced aerogel (16 %), with exception of sample A\_PP\_S\_R1.6 (16 %). Since the one-pot-grafted aerogels are the most flexible materials, they present, in general, high values of elongation at break ( $\sim 30$  %). Sample A\_PD\_S\_R10 shows a particular behavior, as it stood until a very high elongation at break (48 %), although this sample was the stiffest of the reinforced ones (modulus of 848 kPa). The presence of a high amount of polymer (see Sect. 3.3) is the reason for this behavior. Therefore, this confirms that the polymer phase can increase significantly the compression strength (in this case by more than fivefold), while maintaining the flexibility of the materials at the same level, but has a deleterious effect in the bulk density and thermal conductivity (Table 2).

Globally, grafting the aerogels with a polymeric phase improves some of their mechanical properties, but this depends on several factors, like the type and amount of polymer, its distribution in the aerogel and, not less important, the interference that it causes in the silica polycondensation process during gelation.

Because of the ether functional groups, PEG-DA should have created the most flexible aerogels. However, PEG-DA-grafted aerogels feature a smaller Young's modulus only with gel soaking (627 vs. 848 kPa for the PDAEMA-grafted sample), but in one-pot have a slightly higher elongation at break, suggesting good flexibility (33 vs. 30 % for the PDAEMA-grafted sample).

Many authors [7, 9, 13–15] reported grafted silica aerogels that have a modulus in the tens of MPa. In this study, we developed aerogels whose modulus is in the tens of kPa, creating aerogels that are much more flexible. However, these are not yet as flexible as pure MTMS [18] aerogels or as the grafted aerogels reported by Maleki et al. [11], but the latest have bis-silanes in their composition, creating a more open structure with more elastic bonds within the backbone.

### 3.5 Microstructure

SEM images (Fig. 7) reveal spheroid secondary particles with similar size, confirming the existence of the pearl necklace structure (silica network) in all aerogels. In some images, deposits from fragmentation of the particles or from the gold coating can be noticed.

Non-reinforced and gel-soaking-grafted aerogels show a similar pearl necklace structure: particles have a sphere-like shape with similar sizes among them. Moreover, the average particle size seems to be 5  $\mu\text{m}$  for all these aerogels. In spite of TGA showing the existence of polymer in the core of the gel-soaking-grafted aerogels, SEM images show relatively well-defined particles and necks. Thus, the polymer is not noticeable at this level amount, being completely mingled within the structure.

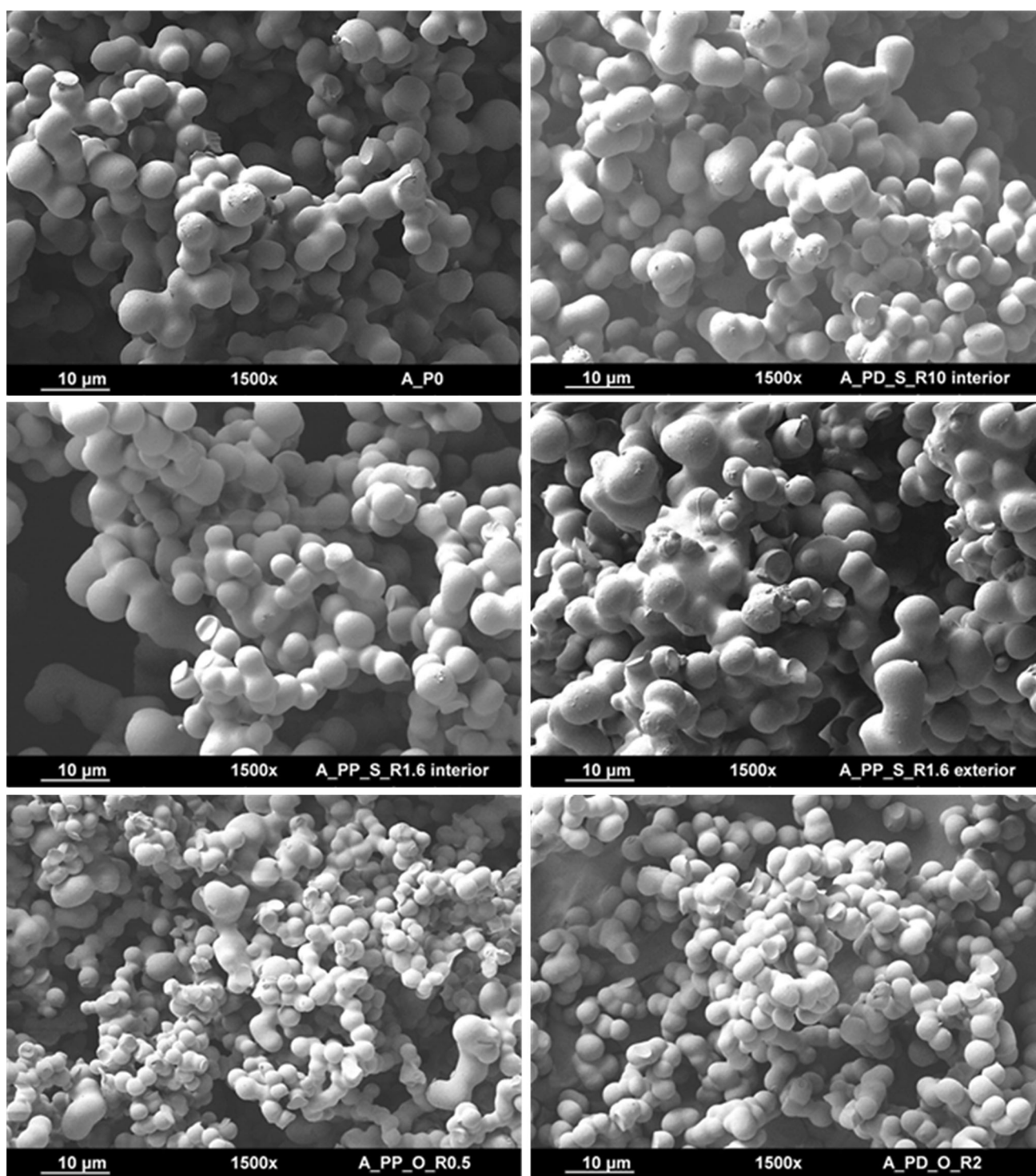


**Fig. 7** SEM micrographs of the aerogel's microstructure

As the TGA revealed significant differences between the core and the outer surface of monoliths grafted through gel soaking, these two parts were also observed by SEM separately. Regardless of the polymer type used for reinforcement, the exterior of the aerogel featured a

heterogeneous surface: in some parts, the surface is very closed and the secondary particles are not individualized, while on others the pearl necklace structure is well defined. As explained earlier, due to the more complete condensation, the outer surface of the gels is more closed than their

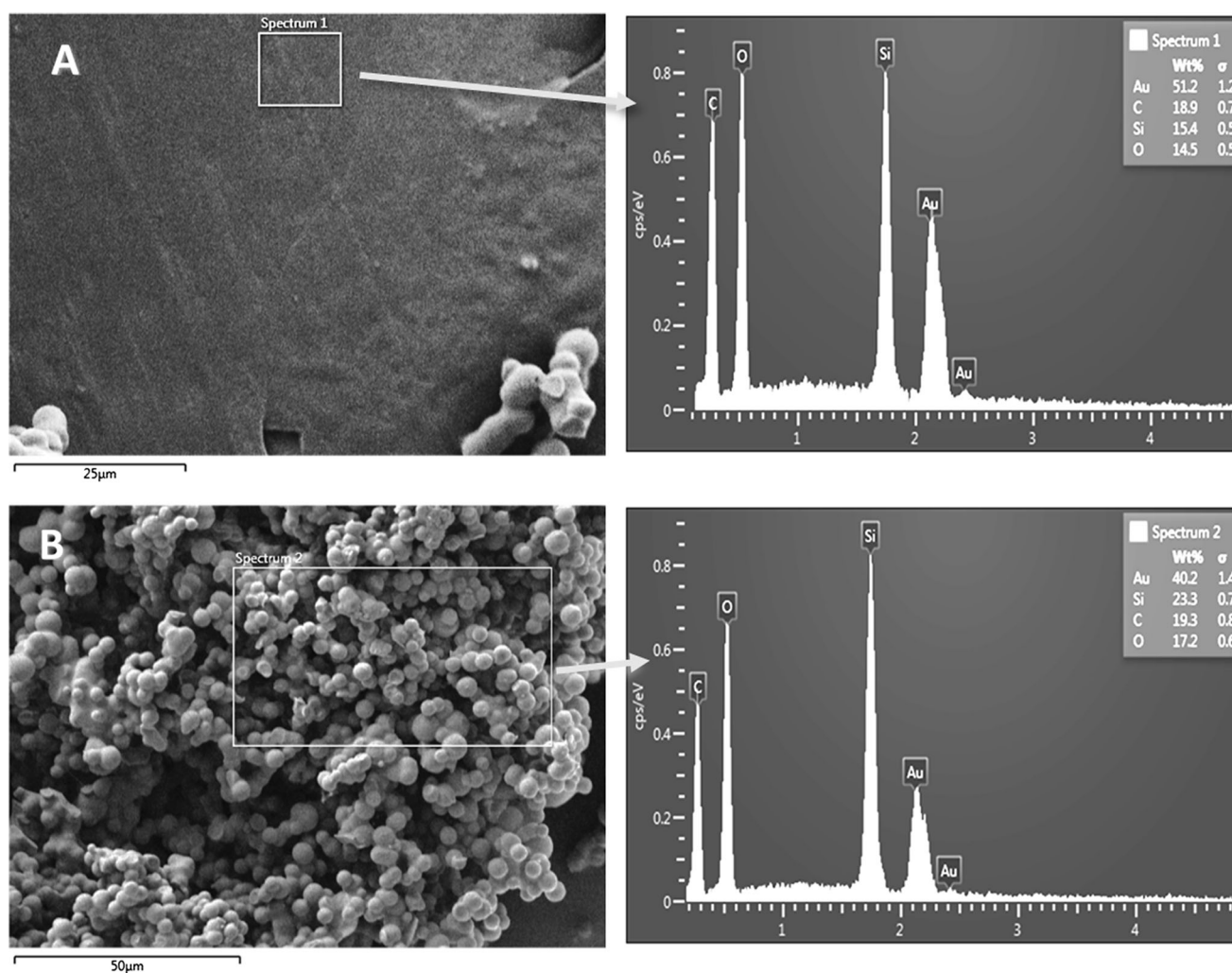


**Fig. 8** EDS analysis of two distinct areas on the outer surface of A\_PP\_S\_R1.6 sample

interior. EDS analysis to this sample (Fig. 8), on each of these very distinct regions, revealed that compared to the average expected elemental composition of the silica backbone, the sites where no individual particles are observed have an excess of oxygen and carbon compared with silicon, and the sites where individual particles are observed feature a similar elemental composition to the one expected on the silica backbone. These results confirm the presence of the polymer in the outer surface, acting as a binder of secondary silica particles. This is in agreement with results obtained by TGA and observations of a more rigid outer layer in the compression tests.

One-pot-grafted aerogels show a very regular pearl necklace structure; the secondary particles are almost spherical and have a narrow size distribution. They are also smaller than the ones from the other aerogels. This very regular microstructure is caused by the porogen effect of the organic moieties during gelation, which controls the particle growth (less extensive condensation) and pore size.

This observation is valid for both polymers, suggesting that the molecular weight of the added macromer and monomer is not a key factor relatively to the particle growth. These samples feature less defined necks and more connections between particles, suggesting a binding effect derived from polymer incorporation.

#### 4 Conclusions

Flexible, hydrophobic and lightweight reinforced aerogels for insulation purposes were prepared. The mixture of TMOS, MTMS and VTMS precursors has shown to be efficient in tailoring the desired flexibility and hydrophobicity onto the final organically modified silica monoliths. The reinforcement, performed with acrylates, was incorporated with the time-consuming gel soaking and streamline one-pot methodologies, in order to allow their comparison.

It has been demonstrated that, in spite of using a monomer or a macromer in the synthesis, both generated similar results, being the major differences between aerogels grafted using different methodologies. We found that gel-soaking-grafted aerogels did not globally present relevant improvements on their properties, being also highly heterogeneous. The effects of monomer/macromer diffusion through the silica backbone were significant in both cases, despite the molecular weight differences. On the contrary, one-pot aerogels showed improvements in almost all evaluated properties, resulting in better heat insulation, lighter, hydrophobic, homogeneous and flexible materials. These improvements are in part due to the effect of the presence of monomers during gelation. So, we conclude that one-pot synthesis is a reliable method for obtaining homogeneous monoliths suitable for insulation purposes. Grafted aerogels became significantly more flexible as Young's modulus decreased by about 10 times when compared to the non-reinforced aerogel. Comparing to other polymer reinforced silica aerogels described in the literature, the ones here studied have shown to be some of the lightest, and with uncommonly low modulus for grafted aerogels.

**Acknowledgments** This work was funded by FEDER funds through the Operational Programme for Competitiveness Factors—COMPETE and National Funds, through FCT—Foundation for Science and Technology under the project PTDC/EQU—EPR/099998/2008—GelSpace—Silica-Based Aerogels for Insulation of Spatial Devices.

## References

- Gurav JL, Jung I-K, Park H-H, Kang ES, Nadargi DY (2010) Silica aerogel: synthesis and applications. *J Nanomater* 2010:1–11. doi:10.1155/2010/409310
- Aegerter MA (2011) Aerogels handbook. In: *Advances in sol-gel derived materials and technologies*. Springer. doi:10.1007/978-1-4419-7589-8
- Durães L, Ochoa M, Rocha N, Patrício R, Duarte N, Redondo V, Portugal A (2012) Effect of the drying conditions on the microstructure of silica based xerogels and aerogels. *J Nanosci Nanotechnol* 12(8):6828–6834. doi:10.1166/jnn.2012.4560
- Soleimani Dorcheh A, Abbasi MH (2008) Silica aerogel; synthesis, properties and characterization. *J Mater Process Technol* 199(1–3):10–26. doi:10.1016/j.jmatprotec.2007.10.060
- Cai JY, Lucas S, Wang LJ, Cao Y (2011) Insulation properties of the monolithic and flexible aerogels prepared at ambient pressure. *Adv Mater Res* 391–392:116–120. doi:10.4028/www.scientific.net/AMR.391-392.116
- Ochoa M, Durães L, Beja A, Portugal A (2012) Study of the suitability of silica based xerogels synthesized using ethyltrimethoxysilane and/or methyltrimethoxysilane precursors for aerospace applications. *J Sol-Gel Sci Technol* 61(1):151–160. doi:10.1007/s10971-011-2604-7
- Randall JP, Meador MA, Jana SC (2011) Tailoring mechanical properties of aerogels for aerospace applications. *ACS Appl Mater Interfaces* 3(3):613–626. doi:10.1021/am200007n
- Maleki H, Durães L, Portugal A (2014) An overview on silica aerogels synthesis and different mechanical reinforcing strategies. *J Non-Cryst Solids* 385:55–74. doi:10.1016/j.jnoncrysol.2013.10.017
- Nguyen BN, Meador MA, Tousley ME, Shonkwiler B, McCorkle L, Scheiman DA, Palczar A (2009) Tailoring elastic properties of silica aerogels cross-linked with polystyrene. *ACS Appl Mater Interfaces* 1(3):621–630. doi:10.1021/am8001617
- Guo H, Nguyen BN, McCorkle LS, Shonkwiler B, Meador MAB (2009) Elastic low density aerogels derived from bis[3-(triethoxysilyl)propyl]disulfide, tetramethylorthosilicate and vinyltrimethoxysilane via a two-step process. *J Mater Chem* 19(47):9054. doi:10.1039/b916355g
- Maleki H, Durães L, Portugal A (2014) Synthesis of lightweight polymer-reinforced silica aerogels with improved mechanical and thermal insulation properties for space applications. *Microporous Mesoporous Mater* 197:116–129. doi:10.1016/j.micromeso.2014.06.003
- Mulik S, Sotiriou-Leventis C, Churu G, Lu H, Leventis N (2008) Cross-linking 3D assemblies of nanoparticles into mechanically strong aerogels by surface-initiated free-radical polymerization. *Chem Mater* 20:5035–5046
- Nguyen BC, Meador MA, Medoro A, Arendt V, Randall J, McCorkle L, Shonkwiler B (2010) Elastic behavior of methyltrimethoxysilane based aerogels reinforced with tri-isocyanate. *ACS Appl Mater Interfaces* 2(5):1430–1443. doi:10.1021/am100081a
- Meador MA, Weber AS, Hindi A, Naumenko M, McCorkle L, Quade D, Vivod SL, Gould GL, White S, Deshpande K (2009) Structure-property relationships in porous 3D nanostructures: epoxy-cross-linked silica aerogels produced using ethanol as the solvent. *ACS Appl Mater Interfaces* 1(4):894–906. doi:10.1021/am900014z
- Meador MAB, Scherzer CM, Vivod SL, Quade D, Nguyen BN (2010) Epoxy reinforced aerogels made using a streamlined process. *ACS Appl Mater Interfaces* 2(7):2162–2168. doi:10.1021/am100422x
- Maleki H, Durães L, Portugal A (2015) Synthesis of mechanically reinforced silica aerogels via surface-initiated reversible addition-fragmentation chain transfer (RAFT) polymerization. *J Mater Chem A* 3(4):1594–1600. doi:10.1039/c4ta05618c
- Vareda J (2015) Smart polymer reinforced silica based aerogels. MSc Thesis, Universidade de Coimbra
- Durães L, Maia A, Portugal A (2015) Effect of additives on the properties of silica based aerogels synthesized from methyltrimethoxysilane (MTMS). *J Supercrit Fluids* 106:85–92. doi:10.1016/j.supflu.2015.06.020
- He Y-L, Xie T (2015) Advances of thermal conductivity models of nanoscale silica aerogel insulation material. *Appl Therm Eng* 81:28–50. doi:10.1016/j.applthermaleng.2015.02.013
- Durães L, Matias T, Patrício R, Portugal A (2013) Silica based aerogel-like materials obtained by quick microwave drying. *Mater Werkst* 44(5):380–385. doi:10.1002/mawe.201300140
- Al-Oweini R, El-Rassy H (2009) Synthesis and characterization by FTIR spectroscopy of silica aerogels prepared using several Si(OR)<sub>4</sub> and R''Si(OR')<sub>3</sub> precursors. *J Mol Struct* 919(1–3):140–145. doi:10.1016/j.molstruc.2008.08.025